CHAPTER

38

Doing more with less: A comparative assessment between morphometric indices and machine learning models for automated gully pattern extraction (A case study: Dashtiari region, Sistan and Baluchestan Province)

Aiding Kornejady[a], *Abbas Goli Jirandeh*[a], *Hadi Alizadeh*[a], *Alireza Sarvarinezhad*[b], *Abdollah Bameri*[b], *Luigi Lombardo*[c], *Christian Conoscenti*[d], *Amir Alizadeh*[a], *Mahdi Karimi*[a], *Mahmood Samadi*[a], *and Esmaeil Silakhori*[a]

[a]Spatial Sciences Innovators Consulting Engineering Company, Tehran, Iran [b]Natural Resources and Watershed Management Organization of Sistan and Baluchestan Province, Zahedan, Iran [c]Faculty of Geo-Information Science and Earth Observation (ITC), University of Twente, Enschede, Netherlands [d]Department of Earth and Marine Sciences (DISTEM), University of Palermo, Palermo, Italy

1 Introduction

Erosion is a global concern that occurs in different forms because of the complex, interlaced connection of different causative factors. Once a raindrop touches the soil surface, water erosion commences, forming a wide range of geomorphological facies.[1] As a common form of water erosion, gullies occur mainly under the interaction of soil chemistry, land use, climate, slope, and the governing hydrological system.[2–4] Large amounts of soils are washed away along the unstable channels characterized as gullies, mostly formed on sparsely vegetated and unprotected lands. Hence, extracting the gully pattern as a substantial part of spatial modeling and, thereby, risk analysis is of prime importance.

Humans have become pattern seekers for their survival and their societal development. In parallel, pattern recognition techniques have undoubtedly obviated that need. To date, different algorithms have been developed to differentiate well the natural patterns, examples of which are supervised and unsupervised machine/deep learning algorithms (ML and DL hereafter) and geographic object-based image analysis (GOBIA).[5–9] However, these techniques operate on big data to attain an acceptable level of success. Particularly for gully delineation, OBIA techniques are a bottom-up trial-and-error optimization technique that entails several object features/variables such as mean, standard deviation, length/width, and the gray level co-occurrence matrix (GLCM) (i.e., frequency of different gray-level pixel combinations in a remotely sensed image).[8] Additionally, GOBIA techniques require a tedious process for learning and prediction/classification tasks. On the other hand, visual interpretation and extraction are cumbersome procedures diluted by boundless human errors and may not be an efficient choice in case of emergency due to the time-consuming procedures involved.

Morphometric indices with singular and multilateral connotations (e.g., topographic, topo-hydrologic, edaphic, and botanic) can signify erosional processes subjected to different runoff mechanisms, especially in areas where lack of data is a major concern. Most morphometric indices are DEM derivatives and follow practical, yet straightforward functions. Many studies have focused on the application of morphometric indices in the context of spatial modeling of different natural hazards, such as landslide susceptibility assessment,[10–12] flood hazard analysis,[13] and gully erosion susceptibility mapping.[14–16] However, the literature review attests that the single use of these indices (i.e., not fed to other standalone models) for automated classification and pattern extraction of natural features has not yet been addressed. Hence, the main idea behind this work is to build a simple yet practical conceptual model based on which different single and combined morphometric indices are used to extract gully boundaries. Compared to the advance and complicated models being used in literature, our proposed framework adopts a back-to-basics routine.

Based on these premises, this study sets out to fill this study gap and test the potential use of morphometric indices for gully pattern extraction, using as a test site the Dashtiari region (Iran). We also took it a step further to compare the results with a powerful family of machine learning models and classification trees and discuss their similarities and differences.

2 Study area

The Dashtiari region is located in Sistan and Baluchestan Province, southeast of Iran (Fig. 1). It lies between the latitudes of 25°41′17″–25°43′10″ N and the longitudes of 60°56′36″–60°59′38″ E. The selected parcel extends for 597.7 ha, 14.2% of which (about 85 ha) is affected by gullies. Elevation ranges between −0.1 and 18.7 m a.s.l. Maximum and minimum precipitations are 125 and 150 mm. Maximum and minimum temperatures fluctuate between 21°C and 35°C. As with many gully-prone areas, massive gullies have deeply incised the entire region of Dashtiari. Silty soil has made the area highly sensitive to erosional processes such that a small amount of rainfall can substantially change the landscape due to discernible longitudinal and lateral extension of gullies. Successively widened and deepened, gullies pose a direct threat to the infrastructures, and casualties are anticipated once they reach the villages. For instance, one of the main gully branches have moved toward the Kajoo stream, the primary water source of residents' drinking and agricultural demands. Once gully branches and streams meet, the gullies' intertwined network will drain out the water and make it out of the locals' reach.

3 Materials and methods

3.1 Data compilation

A DJI Phantom 4 Pro (P4P) V2.0, was used to capture an area of approximately 6 km^2 (Fig. 2), from which 3137 UAV images were acquired and processed using Agisoft Metashape v1.6 and Inpho UASMaster v7.1 image processor tool. Five hours of flight mission with a GSD of 3.88 cm per pixel was accomplished on April 21–22, 2019, based on which an orthophoto and a digital surface model (DSM) with a 15 cm × 15 cm pixel resolution were produced for a Dashtiari parcel, as presented in Fig. 1. Furthermore, Fig. 3 presents two excerpts of the gully branches.

A specialized team of cartographers and photogrammetrists manually drew the gully affected boundaries using 3Dstereo anaglyph glasses, which took approximately 6 months to be completed.

3.2 Morphometric indices

Morphometric indices are valuable DEM derivatives that express indirect connotations of earth processes, such as flood generation mechanisms and erosional features. Hence, they can be useful in areas characterized by a lack of data. In this study, seven morphometric indices, including valley depth (VD), topographic position index (TPI), positive openness (PO), red relief image map (RRIM), elevation, slope degree, and coupled PO-DEM (i.e., multiplication), were purposively selected so that gully patterns could be differentiated and extracted. Table 1 lists the implications of each index. The implementation process was carried out in SAGA-GIS,[17] which offers many useful indices with a straightforward execution process.[18] Additionally, the pixel resolution of the DSM layer was resized to 1 m to expedite the production process of the morphometric indices.

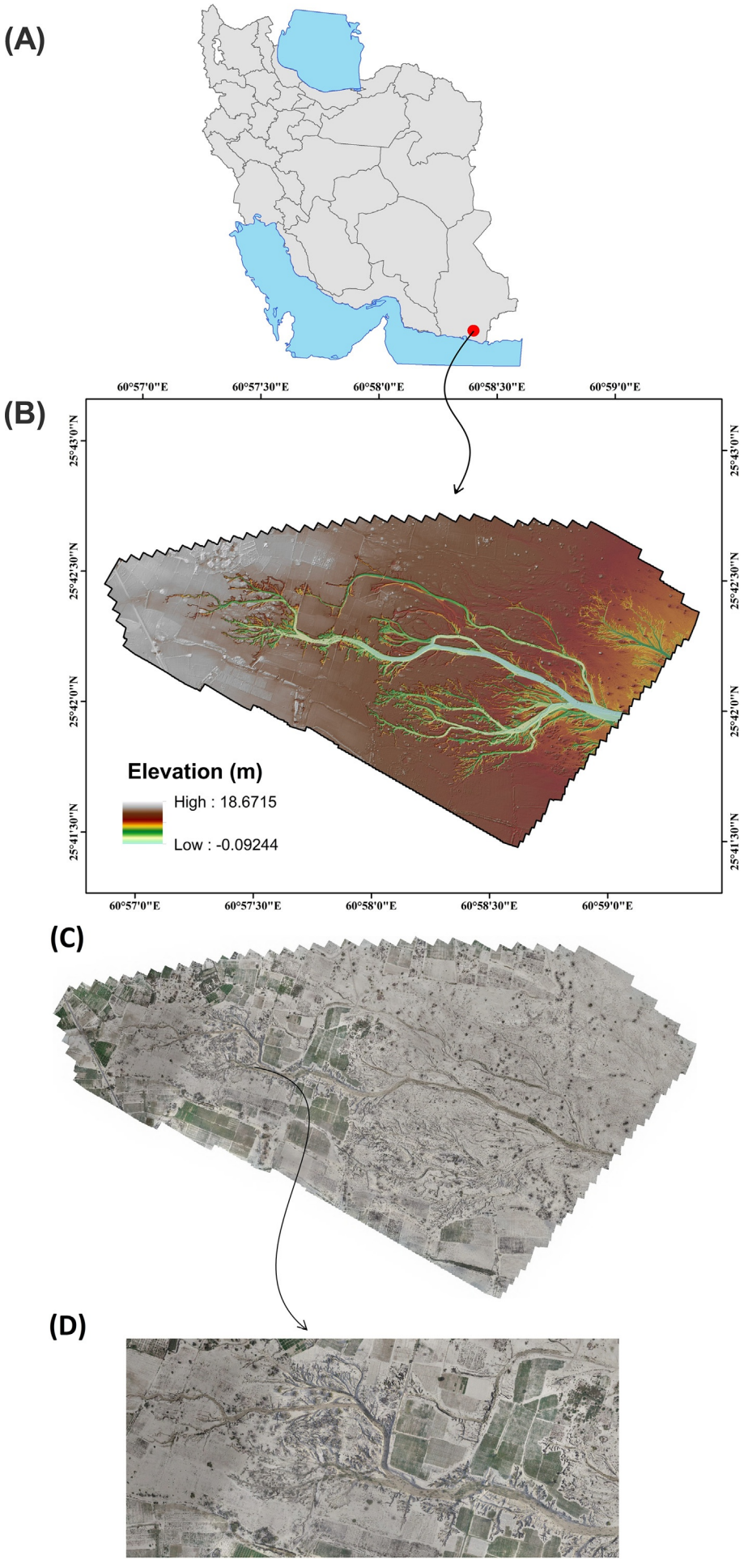

FIG. 1 Location of the study area in Iran (A), UAV-derived digital surface model (B), and the orthophoto of the region (C) with an excerpt site (D).

FIG. 2 Phantom 4 Pro V2.0—DJI.

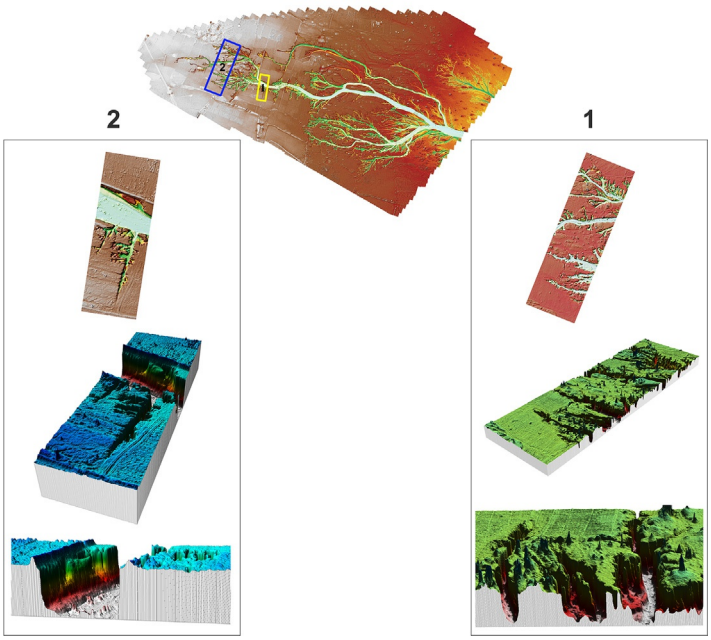

FIG. 3 Cross-sectional excerpts of the gullies sprawled across the Dashtiari region.

TABLE 1 Functional role of the applied morphometric indices for gully pattern extraction.

Factor	Function
Valley depth (VD)	Delineation of ridges from valleys
Topographic position index (TPI)	Delineation of upper, middle, and lower slopes
Positive openness (PO)	Surface concavities from a given zenith
Red relief image map (RRIM)	Effective visualization of subtle topographic features without shading (positive openness-negative openness/2)
Elevation	Differentiating highlands from lowlands
Slope degree	Sudden topographical deflections such as gully edges
Multiplication of PO and DEM (PO-DEM)	A data manipulation technique to incorporate surface concavity and elevation

3.3 Classification tree

In a nutshell, a classification tree (CT) is a way to unifying and classifying the most homogeneous sets from the training samples. To attain this goal, CT adopts different techniques, including splitting, labeling, and pruning. For classification purposes, the process starts with a random binary splitting guess and moves forward to consider different partitions. This is performed through an iterative recursive partitioning process. Each time, the CT algorithm selects the splitting threshold that leads to the largest increase in homogeneity. The Gini index measures such inequality with a fluctuating value between 0 and 1. A Gini value of 1 indicates that each record at the node belongs to a different category, while a Gini value of 0 indicates that all the records at a node belong to the same category.[19] The pruning process removes the leaves and branches that are not used to better predict real cases (unknown classes). The leaves at the root comprise larger records and information and are trained on known classes. Moving forward, the idiosyncrasy of the training records becomes more peculiar to those records and may offer no use for the prediction task. Hence, the CT starts removing the small branches that fail to generalize using the validation dataset. The latter helps the model circumvent the overfitting issue (i.e., being highly accustomed to the training samples such that the model has poor generalization power). More mathematical details can be found in Breiman et al.[19] In this work, the produced morphometric indices and the rasterized training and validation presence:absence samples were used as inputs to the CT model in ModEco software.[20]

3.4 Model training and validation

The Classification of morphometric indices and the employed machine learning model (i.e., CT) both operate in the model training and validation phases. In this regard, machine learning models are specialized in training on partial data (i.e., supervised learning), based on which the model can extract the emerging pattern for the remaining areas in an unsupervised manner (i.e., cast off from the model training phase). Antithetically, the classification of a standalone morphometric index entails finding an optimal threshold, which generally involves trial and error. Hence, we developed a new automated geospatial tool in ArcGIS called the Best Threshold Selector (BTS) to expedite this process. The BTS operates on a pixel-based cross-validation learning scheme in which the raw (unclassified) morphometric index together with the ground truth (presence-absence gully pixels) in the training zone are used as inputs (Fig. 4A). Accordingly, the BTS initiates a recursive threshold-exploring process (Fig. 4B). This process starts with a random guess (50% as a threshold cutoff), whose classification success would be compared to 25% threshold addition (i.e., 75%) and subtraction (i.e., 25%). This process continues until the BTS reaches an unchanged status in the success value (i.e., a plateau). As a rule, BTS consistently follows a direction that leads to a higher success rate.

The success rate corresponds to the so-called optimization goal, represented by three success metrics: true skill statistics (TSS), Area under the receiver operating characteristic curve (AUC), and Cohen's kappa. The tool automatically calculates the optimal threshold value by selecting the desired metric and, accordingly, classifies the morphometric index. For model training and validation, the region was arbitrarily partitioned into two representative areas. In particular, the easternmost part of the region, which is affected by two parallel gully branches, was selected for model training, and the remaining area was kept apart to validate the model results (Fig. 5). Because of the abundance of presence and absence pixels involved in the training and validation stages, obliged to the pixel-based cross-validation technique embedded in BTS, the conventional sample balance issues (i.e., training:validation partitions) are obviated.

3.5 Performance assessment

The performance of the adopted morphometric indices and machine learning model in gully pattern extraction was based on four different metrics: precision, TSS, Cohen's kappa, and Matthews correlation coefficient (MCC). Using four main elements of the confusion matrix (i.e., TP, true positive; TN, true negative; FP, false positive; and FN, false negative), these metrics can assess the performance of models from different aspects.[21–23]

Precision, also termed positive predictive value, is the proportion of correct predictions of presence locations (Eq. 1). As its name implies, precision disregards errors emanating from incorrect predictions of absence locations.

$$\text{Precision} = \frac{\text{TP}}{\text{TP} + \text{FP}} \tag{1}$$

The TSS, referred to as Pierce's skill score, uses more arguments of the confusion matrix, representing the model's ability to distinguish presence from absence (Eq. 2).

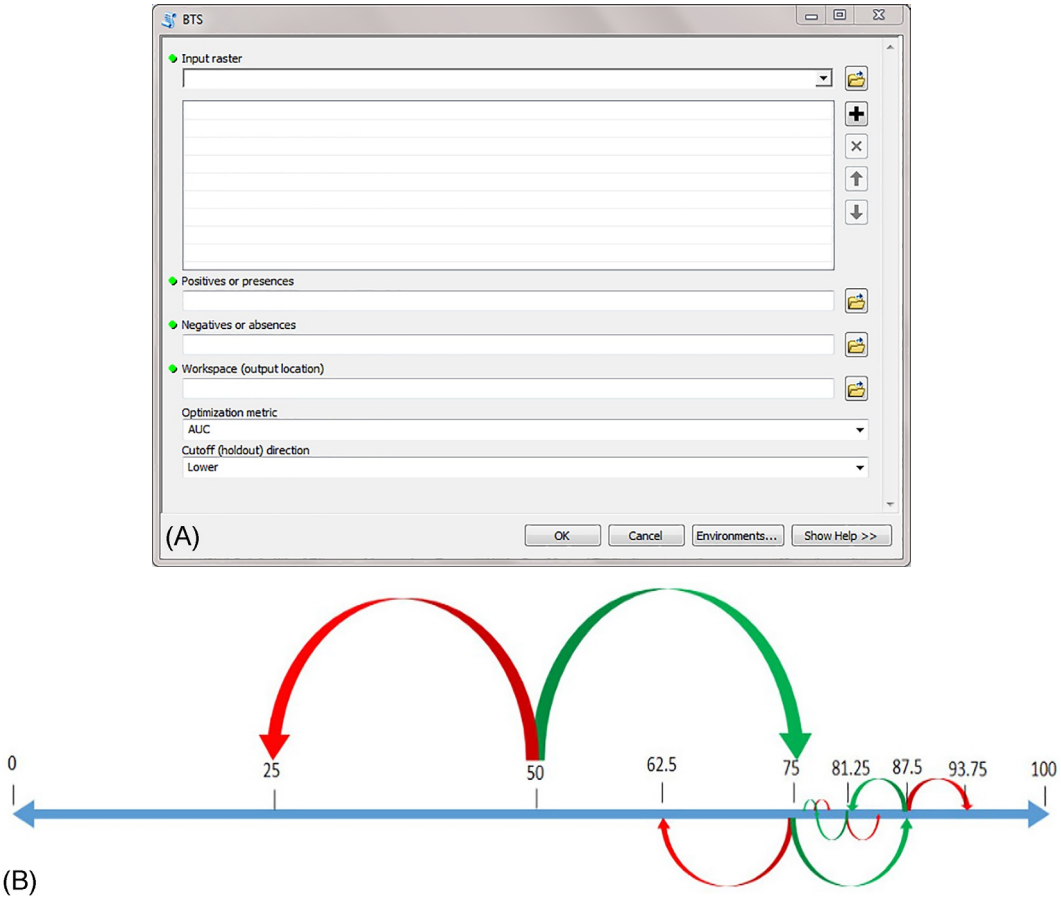

FIG. 4 The graphical user interface of the BTS tool in ArcGIS (A) and the embedded recursive threshold-exploring technique (B—*larger arrows* represent preliminary search steps. *Green arrows*, as opposed to *red ones*, lead to higher success rates).

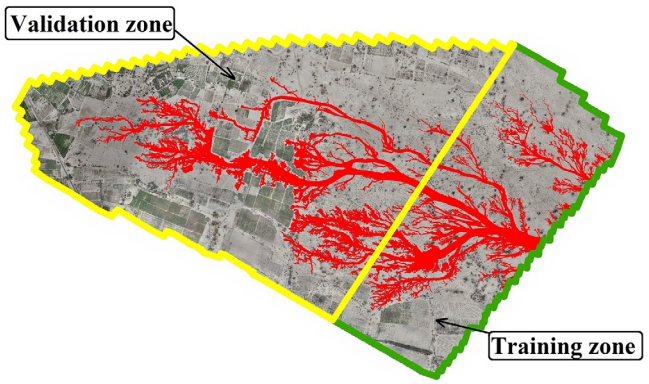

FIG. 5 The selected zones for model training and validation.

$$\mathrm{TSS} = \frac{\mathrm{TP}}{\mathrm{TP}+\mathrm{FN}} - \frac{\mathrm{FP}}{\mathrm{FP}+\mathrm{TN}} = \mathrm{Sensitivity} + \mathrm{Specificity} - 1 \tag{2}$$

Cohen's kappa enables the user to compare the performance of the model for the outcome of random success (Eq. 3).

$$\mathrm{Kappa} = \frac{(\mathrm{TP}+\mathrm{TN}) - [(\mathrm{TP}+\mathrm{FN})(\mathrm{TP}+\mathrm{FP}) + (\mathrm{FN}+\mathrm{TN})(\mathrm{FP}+\mathrm{TN})]/\mathrm{T}}{\mathrm{T} - [\{(\mathrm{TP}+\mathrm{FN})(\mathrm{TP}+\mathrm{FP}) + (\mathrm{FN}+\mathrm{TN})(\mathrm{FP}+\mathrm{TN})\}/\mathrm{T}]} \tag{3}$$

The MCC is a useful correlation coefficient that compares binary classification success, incorporating true and false positive and negative elements (Eq. 4).

$$\mathrm{MCC} = \frac{(\mathrm{TP} \times \mathrm{TN}) - (\mathrm{FP} \times \mathrm{FN})}{\sqrt{(\mathrm{TP} + \mathrm{FP})(\mathrm{TP} + \mathrm{FN})(\mathrm{TN} + \mathrm{FP})(\mathrm{TN} + \mathrm{FN})}} \tag{4}$$

The calculation of the metrics mentioned above was carried out in a modified version of an ArcGIS tool called performance metric tool (PMT). The new version of the PMT is capable of using rasterized samples of presence and absence instead of considering representative point samples. Compared to the older version, PMT-Modified would better reflect the models' true success by creating an all-inclusive matrix of samples. Additionally, PMT-Modified is capable of presenting the elements of the confusion matrix (i.e., TP, TN, FP, and FN) in the form of a raster map to spatially pinpoint the strength of the models (i.e., TP and TN) and weaknesses (i.e., FP and FN).

4 Results and discussion

Fig. 6 presents the classifications derived from morphometric indices (using the BTS tool) and classification trees. A visual comparison between the classification results indicates that all the maps performed well in the training zone,

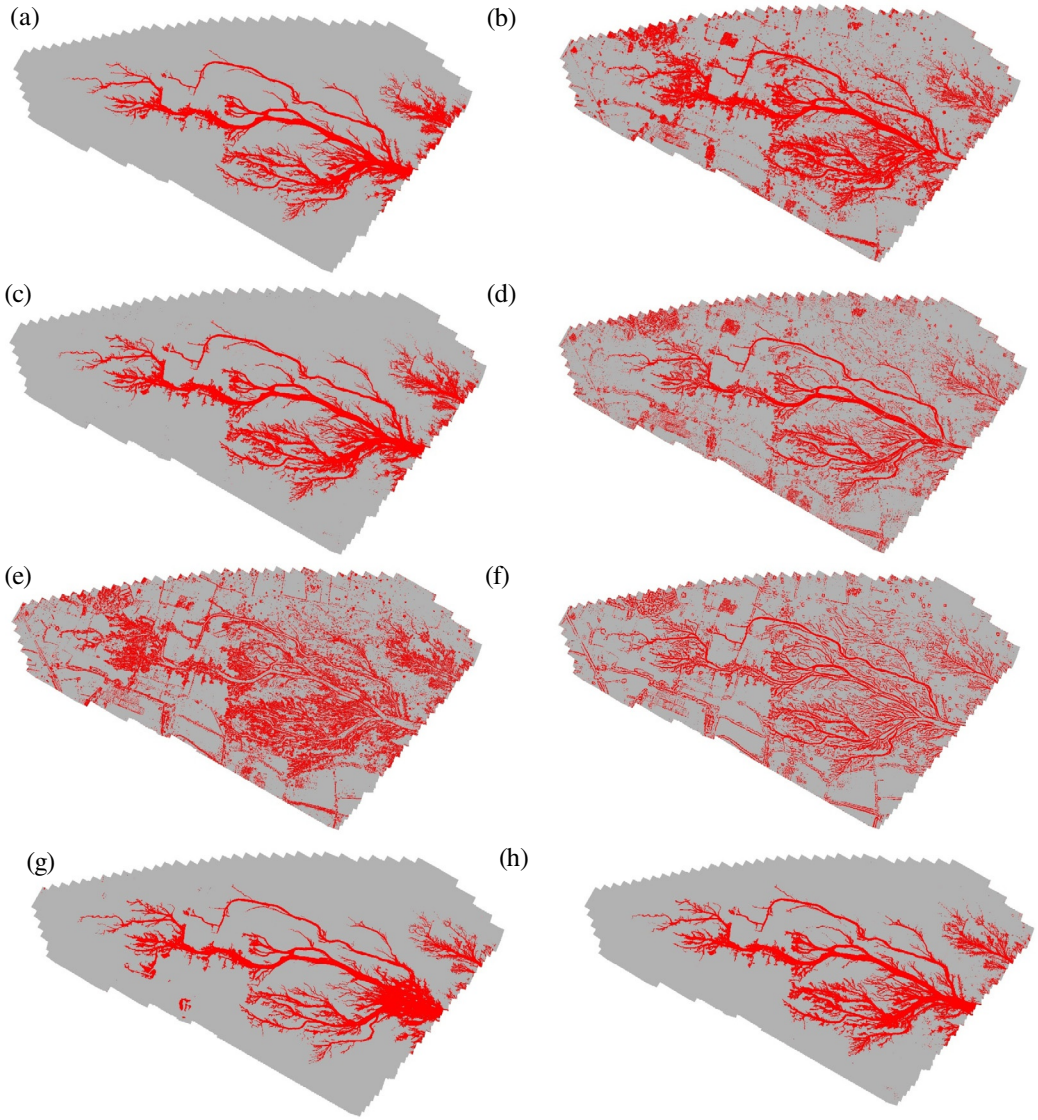

FIG. 6 Gully presence-absence classes derived from morphometric indices (A: DEM, B: positive openness, C: positive openness × DEM, D: RRIM, E: slope, F: TPI, G: valley depth) and classification tree model (H).

while asymmetries became more transparent in the validation zone. From the eight classification maps presented in Fig. 6, it is evident that elevation (DEM), coupled PO-DEM, valley depth, and classification tree performed far better than the other indices. The reason may be the functions presented by each index (Table 1).

Elevation as the main proxy for various morphometric indices may seem highly beneficial for gully extraction, as shown by the classification presented in Fig. 6. However, as previously mentioned, two gully branches with different geometries (i.e., a shallow, less-digitated gully at the upper part and a deep, large gully at the lower part) are discernible in the easternmost sector of the study area, which makes it difficult to assign a single threshold value to each morphometric index. In other words, a single elevation point may not effectively differentiate the gully affected pattern from nongully areas because two gullies with different geometrical features co-exist in the same site. Similarly, valley depth operates on elevation difference and vertical distance to the channel network (referred to as ridge-level interpolation), which explains its small deficiencies. Positive openness represents surface concavities, which not only characterize gullies but also almost anything that exhibits a form of concavity, including a small pit. Hence, conceptualizing the functions each index presented and taking a glance at the gullies together with some trial-and-error factor combination sessions led us to the coupled PO-DEM. The elevation difference helps PO better distinguish gully patterns and exclude small concavities. Testing two arithmetic operations (i.e., addition and multiplication) and investigating the pixel histogram showed that the multiplied PO-DEM exhibits a better breaking point for classification than the added PO-DEM (Fig. 7). In essence, multiplication poses a more restrictive function on the combined indices, while addition creates a relatively smooth map that may not serve best for pattern extraction. On the other hand, the CT also leads to an outstanding classification. Fig. 8 depicts the graphical success and error rates posed by PO, DEM, PO-DEM,

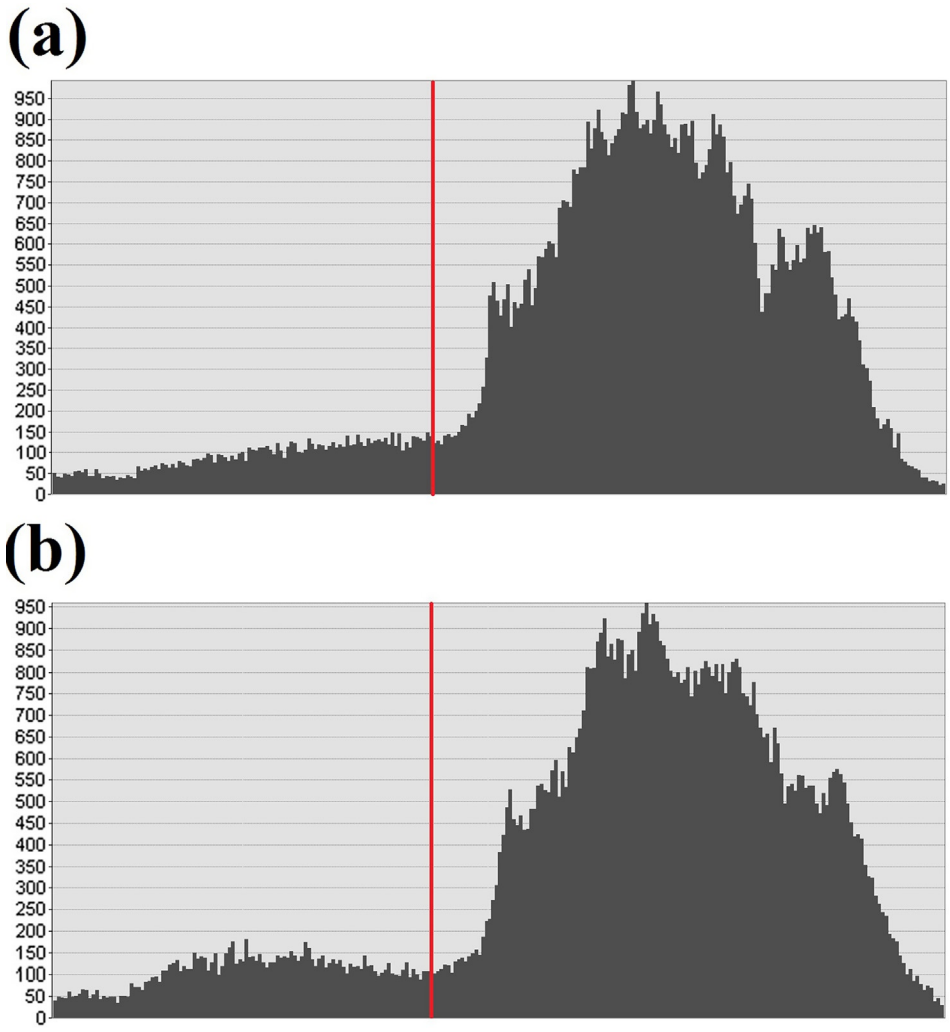

FIG. 7 Histogram created for added PO-DEM (A) and multiplied PO-DEM (B).

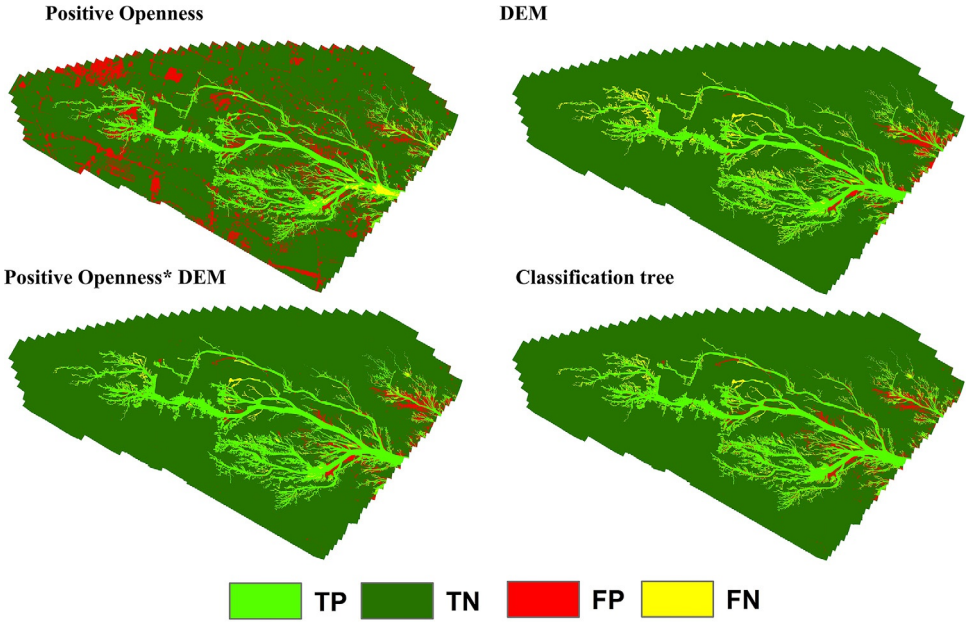

FIG. 8 Calculated true positive (TP), true negative (TN), false positive (FP), and false-negative (FN) values for some of the employed morphometric indices (PO, DEM, and PO × DEM) and the machine learning model (CT) using PMT-modified.

and CT, making it evident that the combination of DEM and PO results in a better gully pattern extraction by reducing the errors encountered in the validation zone.

More dissimilarities between the CT and the well-performing morphometric indices can be derived from the confusion matrix and its derivative performance metrics (Tables 2 and 3, Figs. 9 and 10). The elements of the confusion matrix and the averaged value of the performance metrics are unanimously in line with our previous visual check, based on which PO-DEM, CT, elevation, and valley depth perform better than other indices. More significantly, the PO-DEM that is derived from a simple factor multiplication outperforms a powerful machine learning model, CT.

Although the outstanding performance of PO-DEM is indebted to the automated threshold detection made possible by the BTS tool, the CT follows more complicated recursive training sessions, yet a simple factor combination supersedes its result. In general, a timewise comparison of manually and automatically extracted gully patterns justifies the fact that the latter presents far more promising results. The precision of the extracted gullies using PO-DEM and CT, which may take several minutes to some hours, compared to those manually drawn in 6 months, is beyond expectation. Lastly, this work does not intend to diminish the outstanding results provided by CT. Instead, it encourages the critical role of conceptual models, the merits of simple morphometric indices, and their notable standalone performances, rather than being inputted into complicated black-box models.

TABLE 2 Calculated confusion matrix elements and performance metrics for different employed morphometric indices and machine learning models in the training stage (*bold values* represent the highest performance).

Factor/ Models	Optimal threshold value detected by BTS	Value	Training				Precision	TSS	Cohen's Kappa	MCC	Average
			TP	TN	FP	FN					
PO	75.00	1.45	333,923	1,434,641	215,398	42,068	0.608	0.758	0.6431	0.6625	0.6678
PO_DEM	30.86	9.66	355,124	1,531,949	118,090	20,867	0.751	0.873	0.7937	0.8021	**0.8048**
TPI	41.76	−0.17	259,001	1,499,992	150,047	116,990	0.633	0.598	0.5783	0.5791	0.5971
Valley	37.50	3.95	313,301	1,523,913	126,126	62,690	0.713	0.757	0.7105	0.7139	0.7236
Slope	9.12	7.15	236,656	1,285,795	364,244	139,335	0.394	0.409	0.332	0.3478	0.3706
Elevation	34.90	6.46	332,128	1,552,398	97,641	43,863	0.773	0.824	0.781	0.7838	0.7905
RRIM	43.65	−0.03	272,017	1,526,467	123,572	103,974	0.688	0.649	0.6358	0.6361	0.6520
CT	Self-detected		357,841	1,527,886	122,153	18,150	0.746	0.878	0.793	0.8025	0.8047

TABLE 3 Calculated confusion matrix elements and performance metrics for different employed morphometric indices and machine learning models in the validation stage (*bold values* represent the highest performance).

Factor/ Models	Optimal threshold value detected by BTS	Value	Training				Precision	TSS	Cohen's Kappa	MCC	Average
			TP	TN	FP	FN					
PO	75.00	1.45	466,292	2,992,790	466,958	8492	0.5	0.847	0.598	0.6487	0.6484
PO_DEM	30.86	9.66	414,638	3,443,812	15,936	60,146	0.963	0.869	0.9051	0.9064	**0.9108**
TPI	41.76	−0.17	357,538	3,058,175	401,573	117,246	0.471	0.637	0.5062	0.5258	0.5350
Valley	37.50	3.95	361,922	3,430,942	28,806	112,862	0.926	0.754	0.8163	0.8212	0.8295
Slope	9.12	7.15	340,708	2,816,383	643,365	134,076	0.346	0.532	0.3635	0.3999	0.4103
Elevation	34.90	6.46	344,254	3,455,822	3926	130,530	0.989	0.724	0.818	0.8303	0.8402
RRIM	43.65	−0.03	367,886	3,109,528	350,220	106,898	0.512	0.674	0.5517	0.5681	0.5764
CT	Self-detected		411,425	3,426,648	33,100	63,359	0.926	0.857	0.8812	0.8818	0.8864

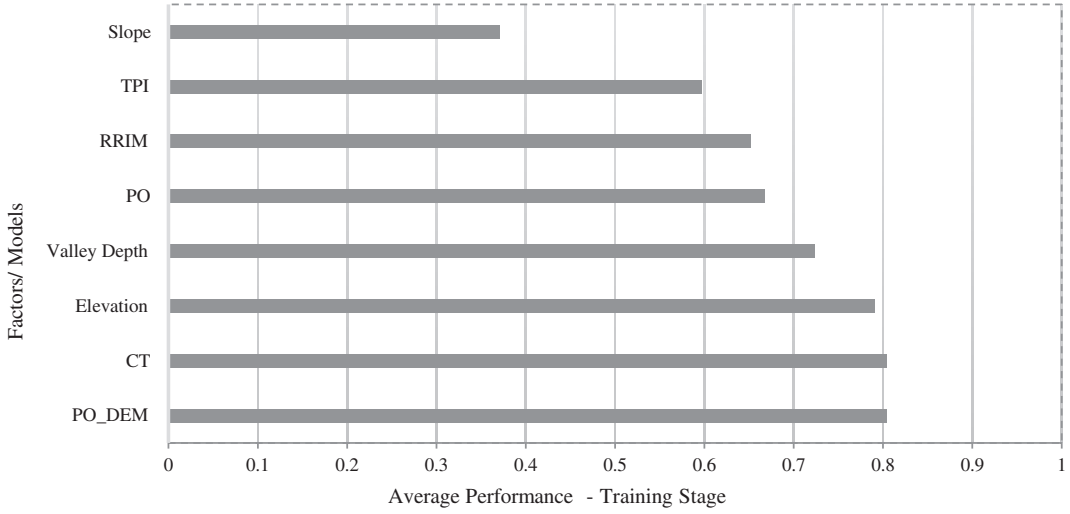

FIG. 9 Average performance of the employed morphometric indices and machine learning models in the training stage.

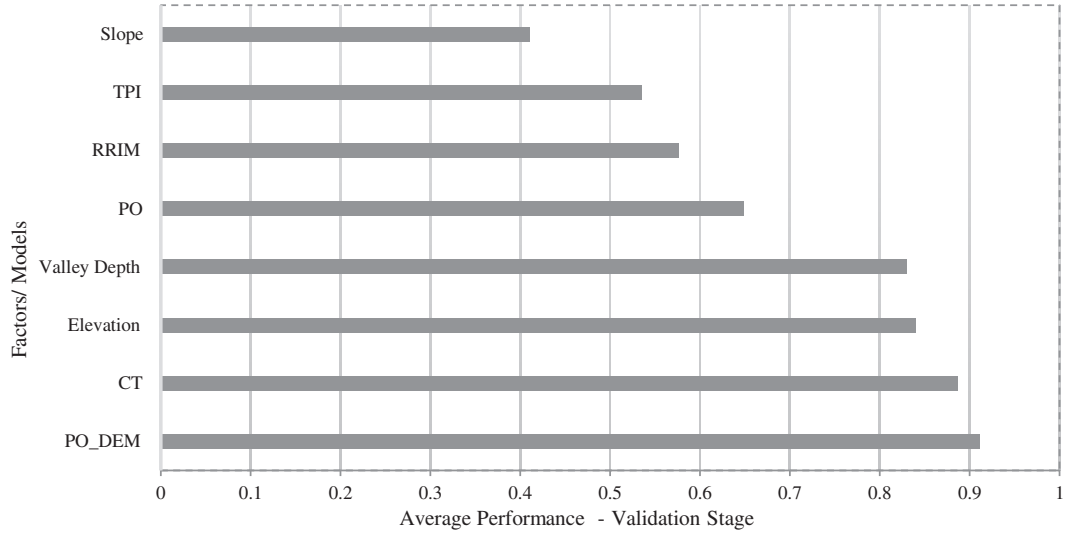

FIG. 10 Average performance of the employed morphometric indices and machine learning models in the validation stage.

5 Comparison, limitations, and future works

Literature review shows that a range of methods has been applied to extract gullies across different areas. Sheshukov et al. tested several compound topographic index models in two paired catchments.[14] Their results attest to the high applicability of topographic indices in extracting the gully patterns, which is in line with our results. Shruthi et al. investigated the application of object-based image analysis techniques for gully delineation.[5] They found that the differences between the gully pattern extracted by OBI methods and the ones manually extracted respectively account for 0.03% and 1.77% for two representative areas. Moreover, they found that gully-related edges are well detected by OBIA methods and can considerably reduce the time spent on manual extraction, which is in complete accordance with our findings. Rahmati et al. also tested the reliability of OBI techniques in gully extraction, which resulted in an overall accuracy value of 92.4%.[8] Phinzi et al. studied the accuracy of machine learning models for gully extraction and found that the random forest and support vector machine models can result in outstanding performance values of 98.7% and 98.01%,[9] which, in accordance with our results, justifies the use of machine learning models in unsupervised feature classification.

In order to give a more reliable factor combination scheme in the Dashtiari region, we would need to apply different techniques (especially OBIA) on the same dataset, which is considered one of the limitations of this work. Additionally, the proposed combined indices (i.e., PO-DEM) should be tested in different areas and gully types. Also, various data configurations and spatial resolution may alter the defined classification thresholds. These points should be addressed and tested in future studies and compared with the findings of this work.

6 Conclusion

This work encourages back-to-basics conceptual modeling using available and straightforward data. Morphometric indices, as simple they may look, can reflect critical hydrological and erosional processes. According to our goal (i.e., gully pattern extraction), the application of morphometric indices was found to be highly beneficial and successful in single-handedly extracting the gully pattern in a short time. Moreover, we presented how knowledge of a phenomenon can help form new and informative factors that would consequently lead to a highly representative model of nature.

The comparative assessment of the coupled positive openness and elevation with a powerful machine learning model justified that a simple factor combination can outperform a complicated machine learning model in terms of both goodness-of-fit and generalization capacity (i.e., prediction). Moreover, the time spent producing PO-DEM or implementing a machine learning model is beyond comparison, considering the 6 months spent on the manual extraction of gullies. Finally, relying on the outstanding precision of morphometric indices in differentiating gully affected from nongully areas, incorporating their results with further manual modifications as a semiautomated procedure may yield the best possible results.

Acknowledgment

We would like to thank Sadaf Amani and Minoo Haghani Shirazi for their meticulous efforts in the manual delineation of gully patterns and data curation.

References

1. Morgan RPC. *Soil Erosion and Conservation.* John Wiley & Sons; 2009.
2. Piest RF, Bradford JM, Spomer RG. Mechanisms of erosion and sediment movement from gullies. In: *Present and Prospective Technology for Predicting Sediment Yields and Sources. Proceeding of Sediment Yield Workshop.* Oxford, Mississippi: USDA sedimentation Lab; 1972:162–176.
3. Chaplot V. Impact of terrain attributes, parent material and soil types on gully erosion. *Geomorphology.* 2013;186:1–11.
4. Day SS, Gran KB, Paola C. Impacts of changing hydrology on permanent gully growth: experimental results. *Hydrol Earth Syst Sci.* 2018;22(6):3261–3273.
5. Shruthi RB, Kerle N, Jetten V. Object-based gully feature extraction using high spatial resolution imagery. *Geomorphology.* 2011;134(3–4):260–268.
6. d'Oleire-Oltmanns S, Eisank C, Dr□gut L, Blaschke T. An object-based workflow to extract landforms at multiple scales from two distinct data types. *IEEE Geosci Remote Sens Lett.* 2013;10(4):947–951.
7. d'Oleire-Oltmanns S, Marzolff I, Tiede D, Blaschke T. Detection of gully-affected areas by applying object-based image analysis (OBIA) in the region of Taroudannt, Morocco. *Remote Sens (Basel).* 2014;6(9):8287–8309.
8. Rahmati O, Tahmasebipour N, Haghizadeh A, Pourghasemi HR, Feizizadeh B. Evaluating the influence of geo-environmental factors on gully erosion in a semi-arid region of Iran: an integrated framework. *Sci Total Environ.* 2017;579:913–927.

9. Phinzi K, Abriha D, Bertalan L, Holb I, Szabó S. Machine learning for gully feature extraction based on a pan-sharpened multispectral image: multiclass vs. binary approach. *ISPRS Int J Geo Inf.* 2020;9(4):252.
10. Kornejady A, Ownegh M, Bahremand A. Landslide susceptibility assessment using maximum entropy model with two different data sampling methods. *Catena.* 2017;152:144–162.
11. Kornejady A, Ownegh M, Rahmati O, Bahremand A. Landslide susceptibility assessment using three bivariate models considering the new topo-hydrological factor: HAND. *Geocarto Int.* 2018;33(11):1155–1185.
12. Lombardo L, Opitz T, Huser R. Numerical recipes for landslide spatial prediction using R-INLA: a step-by-step tutorial. In: *Spatial Modeling in GIS and R for Earth and Environmental Sciences.* Elsevier; 2019:55–83.
13. Choubin B, Moradi E, Golshan M, Adamowski J, Sajedi-Hosseini F, Mosavi A. An ensemble prediction of flood susceptibility using multivariate discriminant analysis, classification and regression trees, and support vector machines. *Sci Total Environ.* 2019;651:2087–2096.
14. Sheshukov AY, Sekaluvu L, Hutchinson SL. Accuracy of topographic index models at identifying ephemeral gully trajectories on agricultural fields. *Geomorphology.* 2018;306:224–234.
15. Garosi Y, Sheklabadi M, Conoscenti C, Pourghasemi HR, Van Oost K. Assessing the performance of GIS-based machine learning models with different accuracy measures for determining susceptibility to gully erosion. *Sci Total Environ.* 2019;664:1117–1132.
16. Conoscenti C, Rotigliano E. Predicting gully occurrence at watershed scale: comparing topographic indices and multivariate statistical models. *Geomorphology.* 2020;359:107123.
17. Conrad O, Bechtel B, Bock M, et al. System for automated geoscientific analyses (SAGA) v. 2.1. 4. *Geosci Model Dev.* 2015;8(7):1991–2007.
18. Olaya V, Conrad O. Geomorphometry in SAGA. *Dev Soil Sci.* 2009;33:293–308.
19. Breiman L, Friedman J, Stone CJ, Olshen RA. *Classification and Regression Trees.* CRC press; 1984.
20. Guo Q, Liu Y. ModEco: an integrated software package for ecological niche modeling. *Ecography.* 2010;33(4):637–642.
21. Benjamini Y, Hochberg Y. Controlling the false discovery rate: a practical and powerful approach to multiple testing. *J R Stat Soc Ser B Methodol.* 1995;57(1):289–300.
22. Powers DM. *Evaluation: From Precision, Recall and F-Measure to ROC, Informedness, Markedness and Correlation*; 2011. http://hdl.handle.net/2328/27165.
23. Rahmati O, Kornejady A, Samadi M, et al. PMT: new analytical framework for automated evaluation of geo-environmental modelling approaches. *Sci Total Environ.* 2019;664:296–311.